Polyhedron 29 (2010) 975–984

Contents lists available at ScienceDirect

Polyhedron

journal homepage: www.elsevier.com/locate/poly

Quantum relativistic investigation about the coordination and bonding effects of different ligands on uranyl complexes

Dayán Páez-Hernández [a,b,*], Rodrigo Ramírez-Tagle [b], Edelsys Codorniu-Hernández [a,c], Luis A. Montero-Cabrera [d], Ramiro Arratia-Pérez [b]

[a] Departamento de Diseño y Síntesis Molecular, Instituto Superior de Tecnologías y Ciencias Aplicadas, Av. Salvador Allende y Luaces, Quinta de los Molinos, Plaza de la Revolución, Ciudad Habana, CP 10600, AP 6163, Cuba
[b] Departamento de Ciencias Químicas, Universidad Andrés Bello, Av. República 275, Santiago, Chile
[c] Department of Chemistry, University of Calgary, 2500 University Drive NW, Calgary, Alberta, Canada T2N1N4
[d] Laboratorio de Química Computacional y Teórica, Facultad de Química, Universidad de la Habana, Zapata e G y Mazón, CP 10400 Ciudad Habana, Cuba

ARTICLE INFO

Article history:
Received 26 August 2009
Accepted 23 November 2009
Available online 26 November 2009

Keywords:
Uranyl
Ligand effect
Relativistic effects
ZORA

ABSTRACT

The coordination and bonding effects of equatorial ligands such as fluoride (F^-), chloride (Cl^-), cyanide (CN^-), isocyanide (NC^-), and carbonate (CO_3^{-2}) on uranyl dication (UO_2^{2+}) has been studied using relativistic density functional theory. The ZORA Hamiltonian was applied for the inclusion of relativistic effects taking into account all the electrons for the optimization and the explicit inclusion of spin–orbit coupling effects. Geometry optimizations including the counterions and frequencies analysis were carried out with PW91 and PBE functional. Solvents effects were considered by using the conductor like screening model (COSMO) for water and acetonitrile. The Time-Dependent Density Functional Theory (TDDFT) was used to calculate the excitation energies with GGA SAOP functional and the electronic transitions were analyzed using double group irreducible representations. The theoretical results are in a good agreement with experimental IR, Raman and EXAFS spectra and previous theoretical results. New information about the effect of different (donor and acceptors) ligands on the bonding of uranyl ion and on the electronic transitions involved in these complexes is provided with a possible impact on the understanding of the uranyl coordination chemistry.

1. Introduction

Actinide complexes have been the subject of several theoretical researches particularly in the last decade [1–29]. Most of them have been devoted to provide some contributions to actinide chemistry relevant to actinide separation, complexes and sequestration in mesoporous materials. These investigations strongly impacts the understanding and prediction of actinide transport in the environment specially related to the safety of nuclear waste repositories [11,30–35]. In general, actinide chemistry is a very active research area and the knowledge of actinide migration in geological and biological environment has crucial importance [33,36–39]. Despite the significant challenge that imply to the theoreticians the accurate description of the electronic structure and solution properties of actinide species, the uranyl ion has been extensively studied by quantum computational methods [1,10,26,29,40]. In inorganic complexes containing heavy atoms such as uranium and plutonium the relativistic effects play an important role [41,42]. They are heavy metals, and in most of the cases, the electronic structure involves a partly filled f-shell, which means that all complexes except the simplest ones will have a complex electronic structure [2–5,43,44]. Furthermore the f-shell is more diffuse than in lanthanide case and it can participate in the bond formation. The chemical behavior of uranium is controlled by the structure and reactivity of an array of ligated complexes and clusters that is derived from competitive influences of 5f, 6d, and 7s orbitals on the metal center [45–47]. Other difficulties for the theoretical approaches have been related with the inclusion of electron–electron interactions, spin–orbit coupling and electron correlation effects which are crucial for the explanation of the chemical behaviors of these compounds. Most of the reported quantum chemical studies of actinides complexes incorporate relativistic effects by using scalar relativistic effective core potential (ECP) approximation, without treating these effects explicitly. They have been focused more on the geometrical parameters than in the electronic effects [45–47].

In the present study we have systematically examined by relativistic density functional theory, the electronic structures, vibrational properties and ligand effects of several uranyl complexes, with chlorine, fluorine, hydroxyl, cyanide, isocyanide and carbonate

* Corresponding author. Address: Departamento de Ciencias Químicas, Universidad Andrés Bello, Av. República 275, Santiago, Chile. Tel.: +56 2 93319038.
E-mail address: d.paezhernandez@yahoo.es (D. Páez-Hernández).

0277-5387/$ - see front matter © 2009 Elsevier Ltd. All rights reserved.
doi:10.1016/j.poly.2009.11.019

as ligands. These have been included as the most common environmental species of uranium [2–4,8–11]. Carbonyl ligand has been additionally studied for comparison with similar ligands. Additionally, the effect of water and acetonitrile as solvents has been considered. All the electrons of the calculated systems and the spin-coupling effects have been included in the optimizations. These high level theoretical results have been compared with experimental IR, Raman and EXAFS spectra. The remainder of this article is organized as follows: in Section 2 we describe the theoretical models and our computational set up with the application of quantum relativistic DFT methods. In Section 3 we summarize our findings, compare them with other theoretical and experimental results and discuss their possible impacts on the understanding of uranyl coordination.

2. Theoretical models and computational details

Ligand steric and electronic properties generally determine the number of atoms that can be included in the equatorial plane of uranyl ion. Pentagonal–bipyramidal geometry is the most common arrangement. However, more sterically demanding ligands (such as heavier halides) tend to induce tetragonal–bipyramidal structures [48–50]. In the present work a number of uranyl complexes with four and five ligands coordinated in equatorial plane were selected. The general formula for these systems is $UO_2(X)_n^{2-q}$ (n = 4,5) where X = Cl^-; F^-; OH^-; CN^-; NC^-; CO and q is the ligand charge. Additionally, the complex with CO_3^{2-} bidentate ligand is also calculated, considering two and three ligands in the equatorial plane, in order to complete the four and six uranium coordinations, respectively.

Rough and intuitive counterion (alkaline metal cations Na^+ and Cs^+) arrangements around complexes are also included in these calculations with the aim of compensate the charge of these particular systems [15,51].

Previous calculations of uranyl complexes incorporated the scalar relativistic effects through the application of the relativistic effective core potential (ECP) approximation where the counterion effects were not explicitly considered [2–6]. This implicit inclusion limits the accuracy calculation of some properties that are strongly affected by spin–orbit coupling. Our aim herein is to present a systematic study of the ligand effects on the uranyl ion, with the explicit inclusion of all the electrons, the scalar relativistic effects and spin–orbit coupling. Therefore, we are providing high level theoretical results for the studied uranyl complexes. All structural and electronic properties were obtained by using the Amsterdam Density Functional (ADF) code [52] where the scalar relativistic and spin–orbit effects were incorporated by the zero order regular approximation (ZORA). All the molecular structures were fully optimized via analytical energy gradient method implemented by Verluis and Ziegler, using the local density approximation (LDA) within the Vosko–Wilk–Nusair parametrization for local exchange correlations [53–55]. GGA (Generalized Gradient Approximation) PW91 and PBE functionals were used. Geometry optimizations including the counterions were calculated by a standard Slater-type-orbital (STO) basis sets with triple-zeta quality double plus polarization functions (TZ2P) for all the atoms [56]. In all cases a frequencies analysis was performed after the geometry optimization, where we obtained only positive frequencies confirming local minima. Three different algorithms were applied for the calculation of the charge distribution: classical Mulliken, Hirshfeld and Voronoi cells (VDD) population analyses. These last methods are based on the electronic density analysis and do not explicitly use the basis functions for the calculation. They proved to be numerically very similar and yield chemically meaningful charges [27,28].

Time-Dependent Density Functional Theory (TDDFT) was employed to calculate the excitation energies. Solvent effects including the counterions were considered as well by a conductor like screening model for real solvents (COSMO), in particular using water and acetonitrile as solvents. We also used the GGA SAOP (Statistical Average of Orbitals Exchange Correlation Potential) functional which was specially designed for the calculation of optical properties. In this case the excitation energies were estimated by spin–orbit time dependent perturbation Density Functional Theory.

In order to establish a coordination preference amongst the studied ligands for the uranyl ion, the coordinations energies have been calculated by the following reaction:

$$UO_2^{2+} + nL^{-q} \rightarrow UO_2L_n^{2-nq} \quad (1)$$

Zero point energy (ZPE) values have been included in the calculations.

The calculations performed by first-principles method lets to obtain accurate excitation energies and oscillator strengths for the calculated complexes. The predictions have been compared with all the available structural and spectroscopic information and new information is now provided about the coordination and bonding effects of different ligands to the uranyl center.

3. Results and discussion

3.1. Geometrical and structural analysis

For all the calculated uranyl complexes a description of the geometrical parameters is presented. These results are compared with theoretical and experimental values previously reported which lets to deduce the capacity of the applied methodology for the accurate prediction of the structural parameters.

3.1.1. Geometry of uranyl halogenated complexes

Fluoride and chloride uranyl complexes were studied considering the extreme geometry reported by Henning et al. [15,21,22] and Grenthe et al. [5,6]. In previous experimental and theoretical analysis (four chloride ligands and four and five fluoride ligands). Geometries for these systems were optimized with D_4h and D_5h symmetry (Fig. 1). For the case of chloride, this symmetry was confirmed by the absorption spectra in acetonitrile reported by Henning et al. [22].

Table 1 shows the geometrical parameters for the uranyl halogenated complexes. The difference obtained between both functionals for the U–O uranyl bond distance for chloride complexes is around 0.02 Å. Only 0.03 Å is the deviation of the PBE functional with respect to the experimental result. U–Cl distances are in excellent correlation with the experimental value with a difference of 0.003 Å. The inclusion of counterions does not affect these geo-

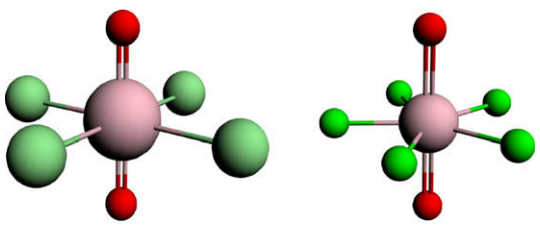

Fig. 1. Uranyl halogenated complexes in D_4h symmetry with U, O, Cl and F atoms denoted in light pink, red and green, respectively. (For interpretation of the references to color in this figure legend, the reader is referred to the web version of this article.)

Table 1
Calculated geometrical parameters of the uranyl halogenated complexes (X = F, Cl). Distances in Å.

Complex	d(U–O_{ax})	d(U–X)
$UO_2Cl_4^{2-}$ (gas)		
PW1	1.812	2.716
PBE	1.810	2.725
$UO_2Cl_4^{2-}$ (acetonitrile)		
PW91	1.818	2.665
PBE	1.803	2.677
K_2 [$UO_2Cl_4^{2-}$] (acetonitrile)		
PW91	1.807	2.691
PBE	1.805	2.692
d(U–K)		
4.339		
Cs_2 [$UO_2Cl_4^{2-}$] (acetonitrile)		
PW91	1.807	2.692
PBE	1.806	2.694
d(U–Cs)		
4.825		
EXAFS/sln [22]	1.77	2.68
$UO_2F_4^{2-}$ (gas)		
PW91	1.854	2.236
PBE	1.852	2.242
$UO_2F_4^{2-}$ (acetonitrile)		
PW91	1.848	2.212
PBE	1.851	2.217
$UO_2F_5^{3-}$ (acetonitrile)		
PW91	1.852	2.225
PBE	1.852	2.226

metrical parameters. U–O uranyl bond distances vary slightly in the presence of solvent effects, while U–Cl distance experiments a variation around 0.05 Å. This effect is related with the instability of more charged systems in the gas phase. For the fluoride complexes similar effects are found. The U–O uranyl bond distance does not suffer any significant variation going from the gas phase to the solvent, neither with the addition of a new ligand. However U–F distances are reduced with the inclusion of the reaction field in 0.03 Å. The difference in U–O uranyl bond distance between four and five coordinate complexes is very small. This is an indicator that a saturation level of the equatorial plane of uranyl ion has been reached and the inclusion of new ligands does not change the geometry of this system. This is supported by some reports that consider the five coordination as an extreme geometry for this system.

Table 2
Charged transfer (CT) obtained for uranyl complexes. $^*CT = 2 - q(U) - 2^*q(O_{ax})$ (q is the atom charge).

Complex	Mulliken	Hirshfeld	Voronoi
$UO_2F_4^{-2}$	0.82	2.38	2.52
$UO_2F_5^{-3}$	1.51	2.74	2.65
$UO_2(CN)_4^{-2}$	1.57	2.01	2.10
$UO_2(NC)_4^{-2}$	1.41	1.97	2.13
$UO_2Cl_4^{-2}$	1.73	2.43	2.34
$UO_2Cl_5^{-3}$	2.02	2.58	2.42
$UO_2(CO_3)_2^{-2}$	1.18	2.00	2.22
$UO_2(CO_3)_3^{-4}$	1.52	2.49	2.53
$UO_2(CO)_4^{+2}$	0.83	1.26	1.61
$UO_2(OH)_4^{-2}$	1.45	2.50	2.62

$^*CT = 2 - q(U) - 2^*q(O_{ax})$, where 2 refers to the isolated uranyl charge, q(U) is the uranium charge in the complex, q(Oax) is the oxygen charge in the complex.

Table 3
Occupation to uranium atomic orbitals in complexes.

Complex	Orbital occupation
U(VI) unligated	$5f^0\ 6s^2\ 6p^6\ 6d^0 7s^0$
$UO_2F_4^{-2}$	$5f^{2.61}\ 6s^2\ 6p^{5.90}\ 6d^{1.38}\ 7s^{0.03}$
$UO_2(CN)_4^{-2}$	$5f^{2.60}\ 6s^2\ 6p^{5.90}\ 6d^{1.59}\ 7s^{0.19}$
$UO_2(NC)_4^{-2}$	$5f^{2.61}\ 6s^2\ 6p^{5.87}\ 6d^{1.53}\ 7s^{0.13}$
$UO_2Cl_4^{-2}$	$5f^{2.71}\ 6s^2\ 6p^{5.83}\ 6d^{1.70}\ 7s^{0.14}$
$UO_2(CO_3)_2^{-2}$	$5f^{2.54}\ 6s^2\ 6p^{5.79}\ 6d^{1.33}\ 7s^{0.07}$
$UO_2(CO_3)_3^{-4}$	$5f^{2.50}\ 6s^2\ 6p^{5.86}\ 6d^{1.46}\ 7s^{0.11}$

The d^0f^0 uranium structure limits the π-back-donation of electrons from the metal center to the ligands. The charge transfer analysis (Table 2) corroborate that the electron donation occurs from the ligands to the metal center. However, Mulliken population analysis does not reproduce this behavior for the case of the tetrafluoride complex. Fluoride is a predominantly π donor ligand but the charge transfer obtained by Mulliken analysis (0.82) is similar to that obtained for $UO_2(CO)_4^{+2}$ (0.83) when it is well known that CO is a π acceptor ligand. Hirshfeld and Voronoi models for charge analysis reproduce better the chemical behavior of these systems, although they give relatively high values for the charge transfer from fluoride to the metal center. Mulliken charges and also its improvements are based on the wave function representation with basis functions and therefore inevitably suffer from the problems of the spatial extent of the basis functions; they are usually centered on a nucleus but will extend over other atomic domains; and the existence of overlap terms, which have to be partitioned over the atoms. When the overlap populations become large, which is the case in large basis sets with diffuse basis functions, the half–half partitioning of the Mulliken population analysis yields totally unphysical charges, which do not properly converge

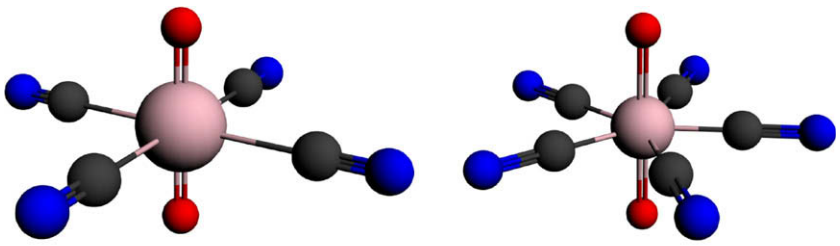

Fig. 2. Uranyl cyanide complexes in D_4h symmetry with U, O, C and N atoms denoted in light pink, red, black and blue, respectively. (For interpretation of the references to color in this figure legend, the reader is referred to the web version of this article.)

Table 4
Calculated geometry parameter of uranyl cyanide and isocyanide complexes (X = C, N). Distances in Å.

Complex	d(U–O_{ax})	d(U–X)	d(C–N)
$UO_2(CN)_4^{-2}$ (gas)	1.804	2.559	1.174
$UO_2(CN)_4^{-2}$ (acetonitrile)			
PW91	1.802	2.535	1.170
PBE	1.803	2.534	1.172
$UO_2(CN)_4^{-2}$ (pyridine)			
PW91	1.802	2.534	1.171
PBE	1.803	2.535	1.172
$UO_2(NC)_4^{-2}$ (gas)	1.803	2.436	1.181
$UO_2(NC)_4^{-2}$ (acetonitrile)			
PW91	1.803	2.414	1.177
PBE	1.803	2.414	1.179
$UO_2(NC)_4^{-2}$ (pyridine)			
PW91	1.803	2.414	1.178
PBE	1.804	2.415	1.179
$UO_2(CN)_5^{-3}$			
PW91 (gas)	1.815	2.588	1.175
PBE (acetonitrile)	1.815	2.579	1.171
Exp. [17]	1.773	2.549–2.577	1.163

with increasing basis set size. Instead the methods based on spatial integration of the deformation density over an atomic domain provide meaningful charges that conform to chemical experience. The spatial integration avoids the problems inherent to basis set based schemes described before [27].

Mulliken analysis reproduces the lowest values amongst the three applied methods for all the studied complexes. For the case of fluoride and chloride complexes, the addition of a new ligand increases the charge transfer. However, in chloride complexes the additional transfer is low due to the steric interaction between five ligands which contribute to destabilize the system. Charge transfer from the ligand to the empty f orbitals is therefore obviously favored. In other words, the interaction between UO_2^{2+} and ligands has some covalent character and it is possible to consider that the coordination energy will be influenced by the charge transfer as well as by the electrostatic and polarization terms [29].

Additionally, in this table, the charge transfer of all the studied complexes is reported which will be used for further comparisons. In Table 3 the orbital occupancies of uranium center are included as well for all the analyzed complexes. It is possible to deduce that the charged transfer is dominant in metal–ligands interaction in all the cases.

3.1.2. Cyanide complexes

Similar to the case of halogenated complexes, cyanide and isocyanide uranyl complexes were studied in D_4h and D_5h symmetries (Fig. 2), based on experimental results reported by Berthet et al. [17]. The structural features of these complexes are presented in Table 4.

In this case the U–O uranyl bond distances and U-ligand distances are in excellent agreement with the experimental results. Although the main interest is to analyze the D_4h geometry, the geometry of $UO_2(CN)_5^{-3}$ complex was calculated as well. These results can be compared with the values published by Berthet et al. in 2006 [17] (Table 4). As it is possible to deduce, the theoretical results are in a good agreement with the experimental values. The comparison of the results obtained for the gas phase with those obtained in solution let us to conclude that the reaction field does not has a significant effect on U–O uranyl bond distances and U-ligand bond distances [57–59]. In general, COSMO model do not produce important changes in geometrical parameters. For isocyanide complex the U–O uranyl bond distance is very similar to cyanide, but U-ligand bond distance is lower in this case.

For f elements the cyano compounds are practically unknown [4,17,19]. Cyanide could be a stronger σ donor or a π acceptor ligand, depending of the reaction medium, although many authors believe that in the case of uranyl ion the donor power is more pronounced [4,19]. This is also supported by the analysis of the charge transfer for these complexes (Table 2). Much controversy has been unleashed about the preference for the coordination of this ligand around uranyl ion. Some theoretical studies have been published in the last decade but the results are not conclusive due to the absence of experimental results. From these high level theoretical results, cyanide complexes might be more stable, although the energetic difference is only 3.33 kcal/mol. A further analysis of the electronic behavior of these complexes is discussed in this work which could contribute with the understanding of these chemical species [4,17,19].

3.1.3. Carbonate complexes

Carbonate is one of the most important ligands in uranyl chemistry. Important experimental and theoretical results have been published about this these complexes. The structures calculated herein are based on previous results reported by Gagliardi et al. [10], Tsushima et al. [14] D_2h and D_3h symmetry were considered for the calculations (Fig. 3).

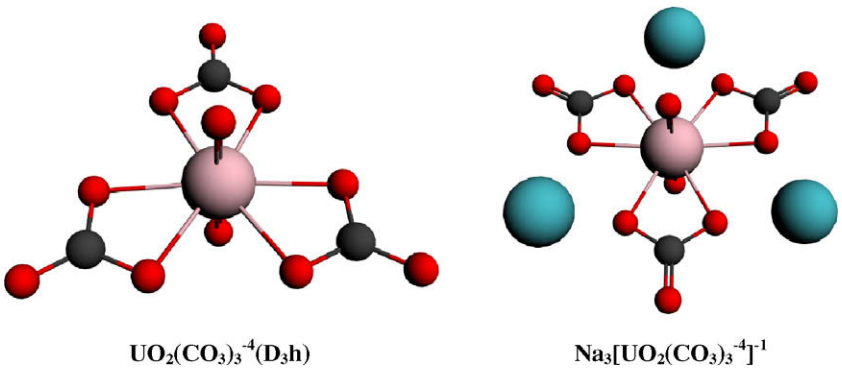

Fig. 3. Uranyl carbonate complex in D_3h symmetry and addition to Na^+ counterion with U, O, C and Na denoted with light pink, red, black and blue, respectively. (For interpretation of the references to color in this figure legend, the reader is referred to the web version of this article.)

Table 5
Comparison of calculated and experimental geometrical parameters of the uranyl carbonate complexes. Distances in Å.

Complex	d(U–O_{ax})	d(U–O_{ec})	d(U–C)	d(U–O)
$UO_2(CO_3)_2^{-2}$				
PBE (gas)	1.833	2.348	2.812	4.057
PBE (water)	1.827	2.358	2.812	4.060
$UO_2(CO_3)_3^{-4}$				
PBE (gas)	1.852	2.538	2.996	4.287
PBE (water)	1.849	2.450	2.903	4.168
$Na_3[UO_2(CO_3)_3]^{-1}$				
PBE (water) d(U–Na) (Å) 3.768	1.832	2.453	2.929	4.179
MBPT2 [10]	1.881	2.407	2.893	4.79
CASPT2 [10]	1.845	–	–	–
EXAFS/sln				
Docrat et al. [60]	1.80 ± 0.02	2.43 ± 0.02	2.89 ± 0.04	4.13 ± 0.04
Ikeda et al. [15]	1.81	2.44	2.92	4.17
EXAFS/solid [61]				
$K_4[UO_2(CO_3)_3]$	1.80	2.43	2.89	4.13
$Ca_2[UO_2(CO_3)_3]$	1.80	2.42	2.88	4.15
$Na_2Ca[UO_2(CO_3)_3]$	1.79	2.43	2.88	4.15

Table 6
Vibrational frequencies calculated for halogenated complexes. All values in cm^{-1}.

Complex	$\nu_s(a_{1g})$	$\nu_a(a_{2u})$	$\delta_d(e_u)$	$\delta_{10}(a_{2u})$
$UO_2Cl_4^{2-}$				
Scalar	815.5	915.4	293.2	111.3
Spin–orbital	812.1	906.7	235.5	103.7
Exp. [42]	838	907	241	107
Cs_2 $[UO_2Cl_4^{2-}]$				
Scalar	817.4	902.6	278.5	113.2
Spin–orbital	812.5	896.0	242.4	104.0
$UO_2F_4^{2-}$				
Scalar	759.3	833.2	411.0	175.8
Spin–orbital	735.0	819.6	388.3	176.8

For this ligand water was considered as the solvent in both cases. Table 5 shows the structural characteristics of the calculated complexes. The uranyl bond distance of 1.849 Å and a U–O carbonate bond distance of 2.450 Å for $UO_2(CO_3)_3^{-4}$ are quite in agreement with the experimental values of 1.81 and 2.44 Å, respectively [15]. In the case of U–O uranyl bond distance, the calculated value is relatively more deviated maybe due to the high charge of this system. For that reason we reoptimized this structure with the addition of Na^+ counterion and obtaining a value 1.832 Å for U–O uranyl bonding distance, which is closer to the

Table 7
Vibrational frequencies calculated for cyanide and isocyanide complexes. All values in cm^{-1}.

Complex	$\nu_s(a_{1g})$	$\nu_a(a_{2u})$	$\delta_b(e_u)$	ν(C–N)(a_{1g})	ν(C–N)(b_{1g})
$UO_2(CN)_4^{-2}$					
Scalar	829.1	921.3	263.07	2110.6	2111.1
Spin–orbit	831.2	915.3	259.01	2121.1	2121.1
$UO_2(NC)_4^{-2}$					
Scalar	825.3	917.3	282.8	2064.1	2053.7
Spin–orbit	831.3	917.4	275.5	2073.6	2063.6

Table 8
Vibrational frequencies calculated for carbonate complexes. All values in cm^{-1}.

Complex	ν_s	ν_a	δ_b	ν_s(C–O)	ν_a(C–O)
$UO_2(CO_3)_2^{-2}$					
Scalar	778.2	845.7	298.3	1593.4	1578.9
Spin–orbit	779.3	846.7	298.6	1587.8	1577.8
$UO_2(CO_3)_3^{-4}$					
Scalar	780.9	860.5	245.6	1527.7	1428.6
Spin–orbit	781.4	865.3	244.5	1538.9	1425.3
Raman/sln [61]	812.5				
Raman/solid [61]		889			
Raman/sln [59,62,64]	812			1545	1460

Table 9
Molecular orbitals splitting in eV for uranyl complexes treated. Values in kcal/mol between parentheses.

Complex	ΔE (eV)
$UO_2(NC)_4^{-2}$	0.10 (2.3)
$UO_2(CN)_4^{-2}$	0.14 (3.2)
$UO_2Cl_4^{-2}$	0.16 (3.7)
$UO_2(CO_3)_3^{-4}$	0.32 (7.4)
$UO_2F_4^{-2}$	0.79 (18.2)

experiment. A comparison with the gas phase results shows that typical U–O distances are shorter in the presence of the reaction field, than in the gas phase. The geometry of the carbonate ligand do not experiment any significant variations with respect to the isolated carbonate.

The geometry of these systems depends on the number of ligands in the equatorial plane of uranyl ion. From the results of Table 5 it is possible to observe that the addition to one ligand increase the U–O uranyl bond distances in 0.02 Å and U–O carbonate in 0.2 Å. It could be owed by the steric interaction among the ligands. The modification of U–O uranyl bond distance is related with the electronic donation from the ligands to the metal center. The charge population analysis (Table 2) reflects an important electronic donation from the ligands, mainly to the f orbitals in the metal center. In the carbonate complexes the electronic back-donation from uranium atoms to the ligands is very low. This explains the relative invariability of carbonate geometry in these complexes compared with the isolated ligand. The charge transfer to the ligands from the uranyl structure can be also analyzed. In our opinion Mulliken population analyses overestimate the ionic character for bonding. For that reason, the electronic donation to uranyl structure obtained with these algorithms is very low compared with the other methods [27].

3.1.4. Frequencies analysis

A frequencies analysis was performed once geometries were optimized for all the uranyl complexes under study. In all cases positive values are obtained for all normal modes which corroborate that minima structures were obtained (Table 6). The frequency values obtained for both approximations are in good correlation with the experimental values, although for halogenated complexes the values of uranyl symmetric vibration are underestimated.

In the cyanide case both methods give similar values for all frequencies and values for cyano and isocyanide complexes. C–N vibration has high values according to Berthet et al. [17] with the absence of electronic π back-donation from the U^{6+} ion to the cyanide ligand (Table 7).

In carbonate complexes the uranyl symmetric vibration is underestimated for both methods with respect to the experimental values, but the others normal modes are good reproduced (Table 8). The symmetric combination of the carbonate C–O are predicted to

Table 10
Characterization of fundamental electronic transition for uranyl complexes. In parenthesis the % of contribution to transition.

Complex	λ_{max} (nm)	f[a]	Contribution	Type transition
$UO_2F_4^{-2}$ (acetonitrile)	267.7	3.70×10^{-3}	$21e_{1/2.g} \rightarrow 17e_{3/2.u}$(83.7) HOMO−3 → LUMO+1 $15e_{3/2.g} \rightarrow 17e_{3/2.u}$(15.0) HOMO−1 → LUMO+1	LMCT
$UO_2(NC)_4^{-2}$ (acetonitrile)	313.4	2.45×10^{-2}	$21e_{1/2.g} \rightarrow 19e_{3/2.u}$ HOMO−5 → LUMO+1	LMCT
$UO_2(CN)_4^{-2}$ (acetonitrile)	320.7	2.07×10^{-2}	$16e_{3/2.g} \rightarrow 19\ e_{3/2.u}$ (52.2) HOMO−6 → LUMO+1 $21e_{1/2.g} \rightarrow 19e_{3/2.u}$(36.7) HOMO−5 → LUMO+1	LMCT
$UO_2(OH)_4^{-2}$ (water)	335.6	2.83×10^{-3}	$35e_{1/2} \rightarrow 38e_{1/2}$ HOMO−2 → LUMO+1	LMCT
$UO_2(CO_3)_3^{-2}$ (water)	435.4	1.74×10^{-3}	$31e_{3/2} \rightarrow 32e_{3/2}$ HOMO → LUMO	LMCT
$UO_2Cl_4^{-2}$ (acetonitrile)	444.7	1.36×10^{-3}	$25e_{1/2.g} \rightarrow 21e_{3/2.u}$(89.2) HOMO−1 → LUMO+1 $24e_{1/2.g} \rightarrow 20\ e_{3/2.u}$(4.9) HOMO−3 → LUMO $19e_{3/2.g} \rightarrow 20e_{3/2.u}$(3.9) HOMO−2 → LUMO $25e_{1/2.g} \rightarrow 20\ e_{3/2.u}$(1.3) HOMO−1 → LUMO	LMCT

[a] Oscillator strength.

be at 1538.9 cm^{-1} and the asymmetric combination at 1425.3 cm^{-1}, both results are in good correspondence with the values obtained with Raman spectroscopy in solution of 1545 and 1460 cm^{-1}, respectively [60,62,63]. A comparative analysis between charge transfers values and uranyl symmetric vibrational frequency can distinguishes a correlation between a decrease in frequency values and the increase of the charge transfer which could be explained by the known fact that the transferred charge reduces the force constant of U–O bonding and consequently the frequency value.

3.1.5. Absorption spectra

The absorption spectra of all the calculated uranyl complexes are provided in this work, which is underlying information for the correct description of optical and geometrical properties of these compounds. This also lets to characterize the uranium speciation in the presence of different ligands. Several experimental data about the absorption spectra has been published for the complexes of uranium with ligands such as chlorine and carbonate but the theoretical incursion in these properties is still poor and lacks of valuable information about the relativistic effects. The absorption spectra provided herein have been calculated by TDDFT and taking into account all the electrons and have included the spin–orbit couplings which modify the common selection rules and lets to get a more depth understanding about the origin and character of the electronic transitions.

The inclusion of spin–orbit coupling produces an important splitting in the molecular orbital diagram for the complexes. In all cases significant values are obtained. These reinforce the need to include the spin–orbit effects in the calculations for these systems with heavy metals. In Table 9 the energetic values to spin–orbit split are presented. These effects produce substantial transformations in absorption spectra for the complexes treated here.

The centrosymmetric coordination of these complexes implies that the spectrum is purely vibronic in nature which means that the light intensity can only be induced by coupling vibration with ungerade symmetry transitions. The symmetric stretching vibration ν_s (a_{1g}) of the uranyl ion itself is always superimposed on each vibronic transition. Besides this gerade vibration, three ungerade, intensity inducing vibration can be coupled to the electronic transitions, namely the asymmetric stretching vibration ν_a (a_{2u}) and the bending vibration ν_b (e_u) of the axial oxygen of the uranyl ion and mainly one vibration of the equatorial ligands ν_{10} (b_{1g}). The U–X out of plane bending b_{1u}, is coupled to the first electronic transition [22,24]. The application of SAOP exchanged correlation potential with spin–orbit effects let us to obtain a significant number of possible transitions for all the studied complexes. Table 10 shows a summary of the most important results.

The most important point group symmetry considered in this contribution is D_4h. For f orbitals the following nomenclature is assumed

$$
\begin{aligned}
5f_0 \quad & 2z^3 - 3z(x^2+y^2) = f_z^3 \\
5f_{\pm1} \quad & (f_{-1} + f_{+1})2xz^2 - x^3 - xy^2 = f_{zx}^2 \\
& (f_{-1} - f_{+1})2yz^2 - y^3 - yx^2 = f_{zy}^2 \\
5f_{\pm2} \quad & (f_{+2} + f_{-2})z(x^2 - y^2) = f_z \\
& (f_{+2} - f_{-2})2xyz = f_{xyz} \\
5f_{\pm3} \quad & (f_{+3} + f_{-3})x^3 - 3xy^2 = f_x \\
& (f_{+3} - f_{-3})3x^2y - y^3 = f_y
\end{aligned}
$$

For chloride complexes the absorption spectra reported in 2005 by Henning et al. [22] present an important band between 380 and 500 nm, with a very vibration fine structure which is quite in agreement with our results. In this case, a transition between 370 and 460 nm with maximum absorption in 444.7 nm is obtained. This absorption band corresponds to the transition between the orbitals HOMO−2(e_{1g}), HOMO−1(a_{2g}) to LUMO (b_{2u}), LUMO+1(b_{1u}). The maximum absorption corresponds to a transition with ligand–metal charge transfer (LMCT) character (Table 11, Fig. 4).

The transition characters are the same for all the studied complexes. The valence orbitals of all the complexes have an important contribution from the ligands. For D_4h symmetry, the ligand atomic orbitals contribute to the formation of molecular orbitals with σ and π symmetry. The symmetry adapted orbitals generate the following irreducible representation for the ligands:

Table 11
Percentage contribution for atomic orbitals to molecular orbitals involved in transition and equivalencies between single and double groups.

MO level	Single group irrep.	Occupation	Double group irrep.	% U	% O	% Total L
$UO_2F_4^{-2}$						
LUMO+2	$6e_{1u}$	0	$E_{3/2u} + E_{1/2u}$	f_x 85.87 f^2_{zx} 3.05	p_x 1.47	p_x 7.86
LUMO+1	$2b_{2u}$	0	$E_{3/2u}$	f_z 94.36	0	p_z 5.15
LUMO	$1b_{1u}$	0	$E_{3/2u}$	f_{xyz} 100	0	0
HOMO	$4a_{2u}$	2	$E_{1/2u}$	f^3_z 34.01 p_z 9.17	p_z 38.93	p_z 17.18
HOMO−1	$2e_{1g}$	4	$E_{3/2g} + E_{1/2g}$	f^2_{zy} 8.63 f_y 1.93	p_y 52.78	p_y 32.72
HOMO−2	$5e_{1u}$	4	$E_{3/2u} + E_{1/2u}$	d_{xz} 2.77	p_x 55.26	p_x 42.04
HOMO−3	$1a_{2g}$	2	$E_{1/2g}$	0	0	p_x 100
$UO_2Cl_4^{-2}$						
LUMO+2	$6e_{1u}$	0	$E_{3/2u} + E_{1/2u}$	f_x 87.45	0	p_x 9.67
LUMO+1	$2b_{1u}$	0	$E_{3/2u}$	f_{xyz} 92.81	0	p_z 5.47
LUMO	$1b_{2u}$	0	$E_{3/2u}$	f_z 99.28	0	0
HOMO	$4a_{2u}$	2	$E_{1/2u}$	f^3_z 20.35 p_z 5.32	p_z 20.84	p_z 55.12
HOMO−1	$1a_{2g}$	2	$E_{1/2g}$	0	p_x 100	0
HOMO−2	$2e_{1g}$	4	$E_{3/2g} + E_{1/2g}$	0	p_z 86.18	p_y 13.71
HOMO−3	$1b_{1g}$	2	$E_{1/2g}$	f_{xyz} 5.88	0	p_z 93.07
$UO_2(CN)_4^{-2}$						
LUMO+2	$7e_{1u}$	0	$E_{3/2u} + E_{1/2u}$	f_x 85.42 f^2_{zx} 1.73 p_x 3.92	0	p_x 5.23 s 3.70
LUMO+1	$1b_{1u}$	0	$E_{3/2u}$	f_{xyz} 99.34	0	0
LUMO	$2b_{2u}$	0	$E_{3/2u}$	f_z 95.46	0	p_z 4.54
HOMO	$6e_{1u}$	4	$E_{3/2u} + E_{1/2u}$	f_y 7.95 p_y 6.73	p_y 3.24	p_y 58.58 s 22.37
HOMO−4	$6a_{1g}$	2	$E_{1/2g}$	d_{z^2} 1.28 s 9.25	p_z 10.37	p_x 57.99 s 8.62
HOMO−5	$3b_{1g}$	4	$E_{1/2g}$	$d_{x^2-y^2}$ 14.04	0	p_y 67.55 s 18.18
HOMO−6	$1b_{2g}$	2	$E_{3/2g}$	d_{xy} 1.22	0	p_x 97.23
$UO_2(NC)_4^{-2}$						
LUMO+1	$2b_{2u}$	0	$E_{3/2u}$	f_z 93.49	0	p_z 6.51
LUMO	$1b_{1u}$	0	$E_{3/2u}$	f_{xyz} 99.29	0	0
HOMO	$6e_{1u}$	4	$E_{3/2u} + E_{1/2u}$	f_y 3.99 p_y 5.55	p_y 1.31	p_y 41.30 s 28.82
HOMO−5	$1a_{2g}$	2	$E_{1/2g}$	0	0	p_x 100
HOMO−6	$1b_{2u}$	2	$E_{3/2u}$	f_z 3.18		p_z 95.05
$UO_2(OH)_4^{-2}$						
LUMO+1	$7a_1$	0	$E_{1/2}$	f_{xyz} 96.15	p_z 1.39	0
LUMO	$2a_2$	0	$E_{1/2}$	f_z 99.31	0	0
HOMO	$1a_2$	2	$E_{3/2}$	0	0	p_x 100
HOMO−1	$7e_1$	4	$E_{3/2} + E_{1/2}$	f_y 2.70 p_y 3.52	p_z 11.02	p_x 81.75
HOMO−2	$6b_2$	2	$E_{1/2}$	f^3_z 6.59 p_z 9.23	p_x 3.94	p_z 50.19
$UO_2(CO_3)_3^{-2}$						
LUMO+1	$5e''_1$	0	$E_{3/2} + E_{1/2}$	f_x 100	0	0
LUMO	$9a'_1$	0	$E_{3/2}$	f_{xyz} 95.14	p_z 3.01	0
HOMO	$11e'_1$	4	$E_{3/2} + E_{5/2}$	d_{xy} 2.53	p_z 1.46	p_x 95.17
HOMO−1	$4a'_2$	2	$E_{1/2}$	f_y 13.14	0	p_x 57.34 p_y 29.96

$\Gamma_\sigma s = E_u + A_{1g} + B_{1g}$
$\Gamma_\sigma p_x = E_u + A_{1g} + B_{1g}$
$\Gamma_\pi p_y = E_u + A_{1g} + B_{1g}$
$\Gamma_\pi p_z = E_u + A_{2u} + B_{1u}$

In chloride and fluoride complexes, the HOMO ($4a_{2u}$) and b_{1u}, b_{2u} molecular orbitals are primarily ligand based molecular orbitals resulting from the p_z, p_x symmetry adapted orbitals with the participation of fo, f_z and f_{xyz} uranium atomic orbitals. In orbitals with gerade parity, the participation of f orbitals is very low. The electronic transition occurs from these orbitals to the empty orbitals with high contribution of uranium f orbitals (Fig. 4). Table 11 shows the representation of the electronic transitions in the studied complexes with the respective equivalences between single and double group representations. For chloride complexes also six other wave length were obtained in a good agreement with the absorption spectra reported by Henning el al. [22].

For cyanide complexes, the origin of transitions and nature of orbitals involved in excitations and the wave length of the maximum absorption are similar for both cases. In the isocyanide complex the maximum wave length is slightly lower than in the cyanide ones. In this case the orbitals involved in these transitions

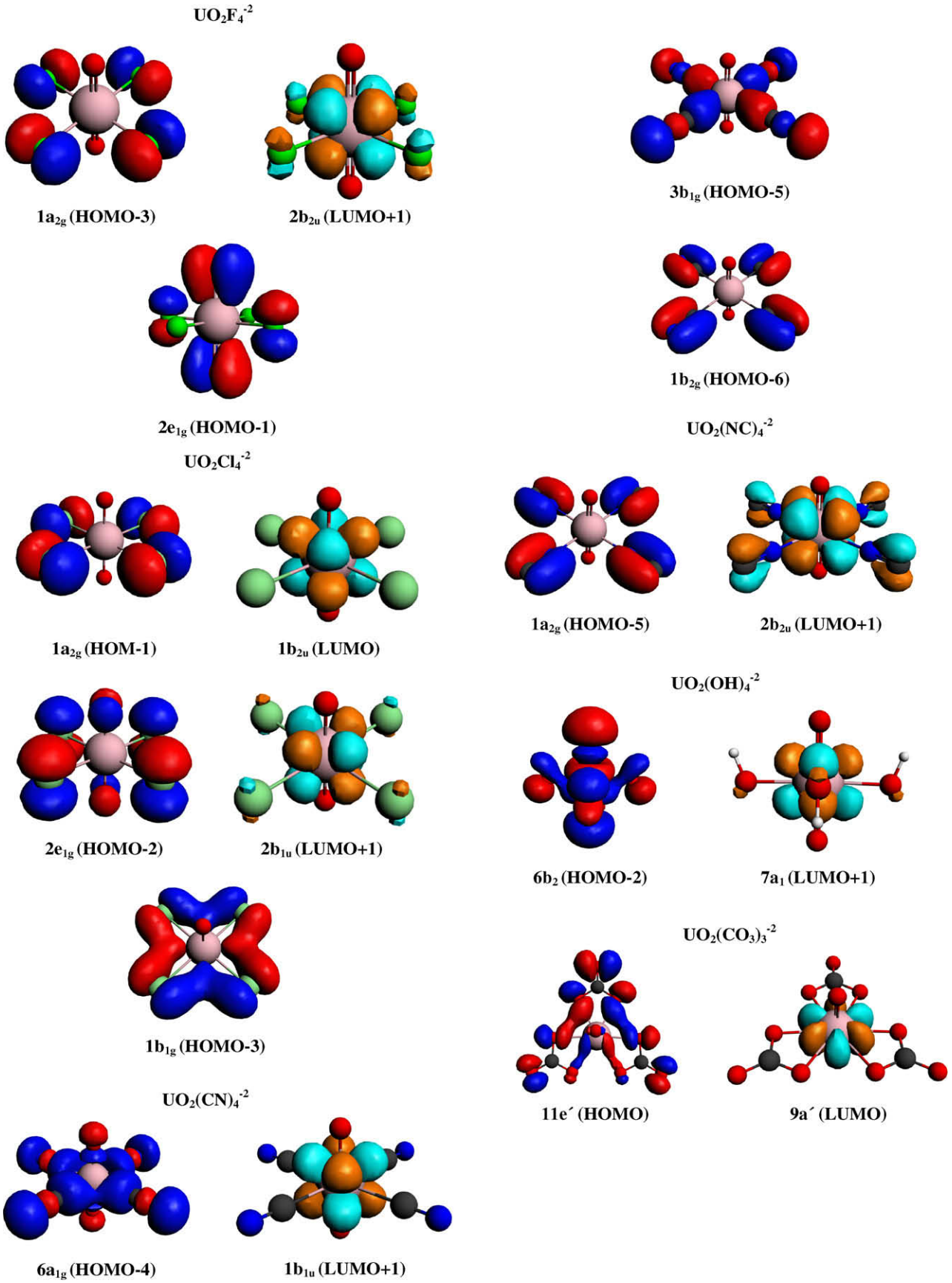

Fig. 4. Selected molecular orbitals involved in electronic transitions plotted at an isovalue 0.025.

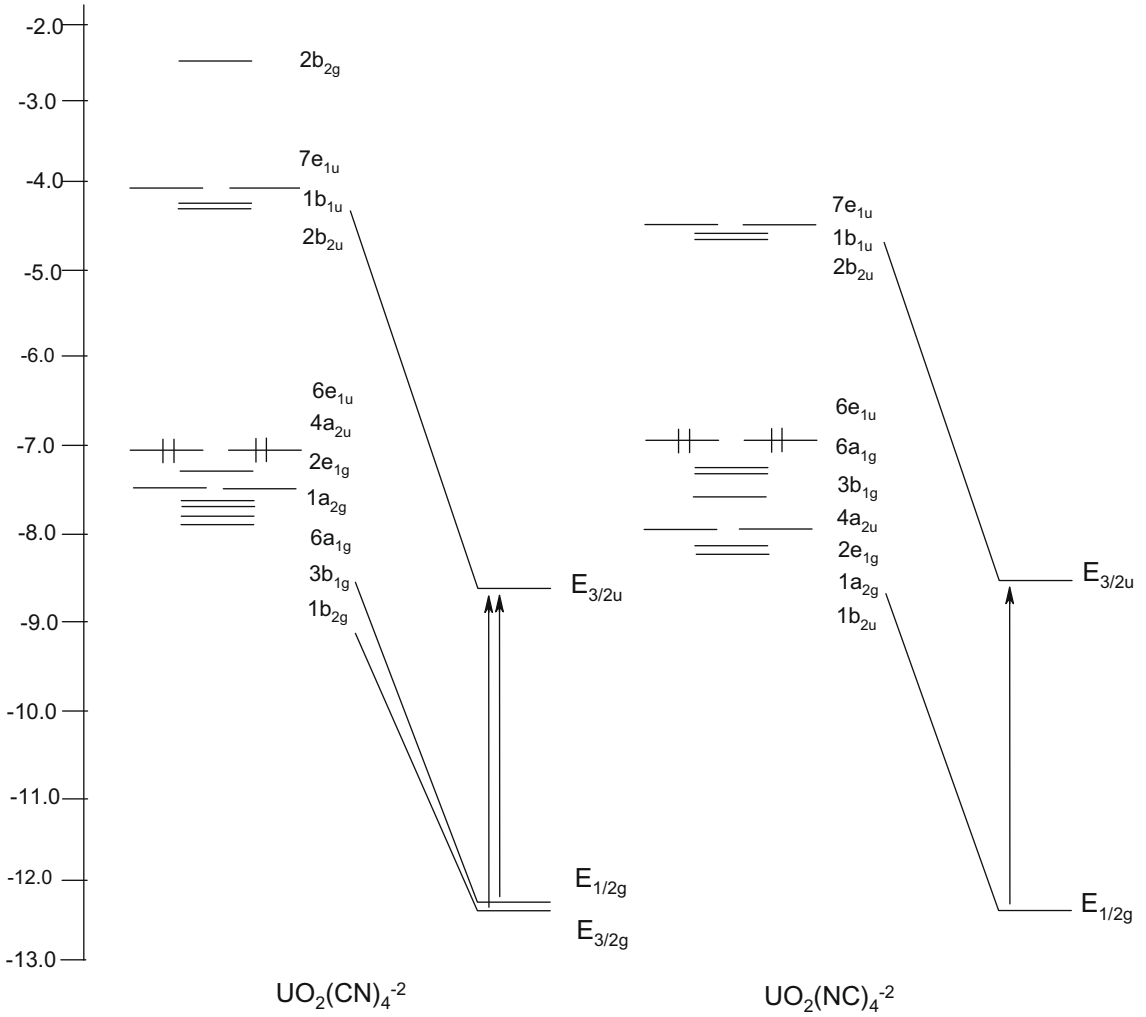

Fig. 5. Uranyl cyanide and isocyanide molecular orbitals diagram. The origin of transition in double group representation is presented.

Table 12
Reaction energy values (kcal/mol) for uranyl complexes (ZPE correction included).

Complex	ΔE (gas)	ΔE (solution)
$UO_2F_4^{-2}$	−702.8	−188.4
$UO_2Cl_4^{-2}$	−572.1	−150.9
$K_2[UO_2Cl_4^{-2}]$		−194.2
$Cs_2[UO_2Cl_4^{-2}]$	–	−178.2
$UO_2(CN)_4^{-2}$	−551.1	−133.5
$UO_2(NC)_4^{-2}$	−597.9	−130.6
$UO_2(CO_3)_2^{-2}$	−834.5	−166.3
$UO_2(CO_3)_3^{-4}$	−661.1	−197.1
$Na_3[UO_2(CO_3)_3^{-4}]$	–	−313.4
$UO_2(OH)_4^{-2}$	−708.7	−242.3

are HOMO−6, HOMO−5 and LUMO+1. The transition characters are similar to the halogenated complexes. The charge transfer occurs from the ligands to the metal center, in particular from $1b_{2g}$, $3b_{1g}$ orbitals with σ and π symmetry, respectively and an important contribution from p_x and p_y atomic orbitals of the ligands to the $1b_{1u}$ and $2b_{2u}$ molecular orbitals, with high contribution to f_{xyz} and f_z uranium atomic orbitals. Fig. 5 shows the electronic distribution diagram of two complexes and include the origin of transition with double group arguments. As can be seen the inclusion of spin–orbit coupling produce an important stabilization of the molecular orbitals.

For carbonate complex in D_{3h} symmetry the character of a transition are the same already seen in the previous cases. The maximum absorption is obtained for a transition from HOMO ($11e'_1$) to LUMO ($9a'_1$) molecular orbitals. The obtained value of 435.4 nm agrees with the experimental value of 450 nm [15]. The HOMO posses π symmetry and is formed fundamentally by the contribution of p_x atomic orbitals from the ligands while the LUMO is formed by the contribution of f_{xyz} atomic orbital from uranium.

Tables 8 and 9 also include the absorption spectra of $UO_2(OH)_4^{-2}$ in D_2d symmetry. This geometry has been reported as the most stable in the literature for hydroxylated uranyl complexes. For that complex transition character coincides with the other calculated complexes (charge transfer from the ligands to the metal center) and the orbitals involved in the electronic transitions are also equivalents.

3.1.6. Thermodynamic stability of uranyl complexes

In order to establish a coordination preference amongst the studied ligands for uranyl ion, the coordinations energies have been calculated by Eq. (1). Table 12 shows the energetic values for both the gas phase and in solution. For the gas phase the thermodynamic stability of theses complexes follows this order: $CO_3^{2-} > OH^- > F^- > NC^- > Cl^- > CN^-$. The coordination energy values are in the range between −830 and −550 kcal/mol which agrees with the results reported by Sarrio et al. [29] for the high

stability of $UO_2(NC)_2$ and $UO_2(CN)_2$ in the same order of our results for the gas phase. Similar results were obtained by Sonnenberg et al. [4] for tatracyanide complexes. However, when solvent effects are included in the calculations the stability order differs with respect to the gas phase results ($OH^- > F^- > CO_3^{2-} > Cl^- > NC^- > CN^-$). Again the cyanide complexes are reproduced as the most stable with respect to isocyanide in agreement with the experimental data. The energy values are less exothermic than in the gas phase. This order is in closer relation with the charge transfer from the ligands to the metal center and confirms that Mulliken analysis definitively does not reproduce correctly the charge distribution of fluoride uranyl complex. Additionally we include the energy values for chloride and carbonate complexes with the respective counterions. In the three cases reported herein the addition of counterions produce an additional stability to the uranyl complexes.

4. Conclusions

The results of this theoretical modeling of uranyl complexes clearly indicate that relativistic density functional theory is not only useful for the prediction of geometries of uranyl complexes; it is also a powerful tool in the description of vibration and absorption spectra for these systems. The application of the ZORA Hamiltonian whit the explicit inclusion of spin–obit coupling effects reproduces geometries and vibration frequencies in good agreement with experimental results and in close relation with geometry results reported in previous theoretical works. The absorption spectra of all the calculated uranyl complexes are provided in this work with a detailed description of the electronic transitions involved. In all cases the more intense transition mean a charge transfer from ligands to the metal center (TCLM). The analysis of bonding nature shows that charge transfers play an important role in metal–ligand coordination which is also supported by the energy analysis. The coordination and bonding effects of the different studied ligands on uranyl complexes obtained in this work would be a good contribution to the understanding of uranium chemistry in its release to ground or superficial waters from waste repositories. The inclusion of spin–orbit effects plays a central role in the correct description of these properties.

Acknowledgement

We thank to following projects UNAB DI-04-06/I, DI-42-06/R, FONDECYT 1070345, Postdoctoral FONDECYT 3100048 and Millennium Nucleus P07-006-F.

Appendix A. Supplementary data

Supplementary data associated with this article can be found, in the online version, at doi:10.1016/j.poly.2009.11.019.

References

[1] P. Pyykko, J. Li, N. Runeberg, J. Phys. Chem. 98 (1994) 4809.
[2] G. Schreckenbach, P.J. Hay, R.L. Martin, J. Comput. Chem. 20 (1999) 70.
[3] G. Schreckenbach, J. Hay, R.L. Martin, Inorg. Chem. 37 (1998) 4442.
[4] J.L. Sonnenberg, P.J. Hay, R.L. Martin, B.E. Bursten, Inorg. Chem. 44 (2005) 2255.
[5] V. Vallet, U. Walhgren, B. Schimmelfenning, H. Moll, Z. Szabó, I. Grenthe, Inorg. Chem. 40 (2001) 3516.
[6] U. Walhgren, H. Moll, I. Grenthe, J. Phys. Chem. 103 (1999) 8257.
[7] V. Vallet, U. Wahlgren, Z. Schimmelpfenning, Z. Szabo, I. Grenthe, J. Am. Chem. Soc. 123 (2001) 11999.
[8] L. Gagliardi, P. Pykko, J. Phys. Chem. 106 (2002) 4690.
[9] L. Gagliardi, P. Pykko, Angew. Chem. 43 (2004) 1573.
[10] L. Gagliardi, I. Grenthe, B.O. Roos, Inorg. Chem. 40 (2001) 2976.
[11] D.L. Clark, D.E. Hobart, M.P. Neu, Chem. Rev. 95 (1995) 25.
[12] V. Vallet, U. Wahlgren, Z. Szabo, I. Grenthe, Inorg. Chem. 41 (2002) 5623.
[13] Z. Szabo, J. Glaser, I. grenthe, Inorg. Chem. 35 (1996) 2036.
[14] K. Mizuoka, S. Tsushima, M. Hasegawa, T. Hoshi, Y. Ikeda, Inorg. Chem 44 (2005) 6211.
[15] A. Ikeda, Ch. Henning, S. Tsushima, K. Takao, Y. Ikeda, A.C. Scheinost, G. Bernhard, Inorg. Chem. 46 (2007) 4212.
[16] W.A. Jong, E. Apra, T.L. Windus, J.A. Nichols, J. Harrison, K.E. Gutowski, D.A. Dixon, J. Phys. Chem. A 109 (2005) 11568.
[17] J.C. Berthet, P. Thuery, M. Ephritikhine, Chem. Commun. (2007) 604.
[18] J. Maynadie, J.C. Berthet, P. Thuery, M. Ephritikhine, J. Am. Chem. Soc. 128 (2006) 1082.
[19] N.I. Tarrat, N. Barros, C.J. Marsden, L. Maron, Chem. Eur. J. 14 (2008) 2093.
[20] C. Gaillard, A. Azzi, I. Billard, H. Bolvin, Ch. Hennig, Inorg. Chem. 44 (2005) 852.
[21] Ch. Hennig, K. Servaes, P. Nockemann, K. Van Hecke, L. Van Meervelt, J. Wouters, L. Fluyt, Ch.G. Warland, R. Van Deun, Inorg. Chem. 47 (2008) 2987.
[22] K. Servaes, Ch. Henning, R. Van Deun, Ch.G. Walgrand, Inorg. Chem. 44 (2005) 7705.
[23] M. Buhl, N. Sieffert, V. Golubnychiy, G. Wipff, J. Phys. Chem. A 112 (2008) 2428.
[24] P. Nockemann, K. Servaes, R. Van Deun, K. Van Hecke, L. Van Meervelt, K. Binnemans, Ch.G. Warland, Inorg. Chem. 46 (2007) 11335.
[25] X. Wang, L. Andrews, Inorg. Chem. 45 (2006) 4157.
[26] R.G. Denning, J. Phys. Chem. A 111 (2007) 4125.
[27] C.F. Guerra, J.W. Handgraaf, E.J. Baerends, F.M. Bickelhaup, J. Comput. Chem. 25 (2004) 189.
[28] R.F. Nalewajski, Phys. Chem. Chem. Phys. 4 (2002) 1710.
[29] C.C. Sarrio, S. Hoyau, N. Ismaail, C.J. Marsden, J. Phys. Chem. A 107 (2003) 4515.
[30] B. Vilchis, Y. Meäs, A. Rojas Hernández, Radiochim. Acta 64 (1994) 99.
[31] R. Zarki, A. Elyahyaoui, A. Chiadli, Appl. Radiat. Isot. 55 (2001) 167.
[32] J.L. Ferrero Calabuig, F. Vera Tomé, A. Martín Sánchez, C. Roldán-García, M.F. da Silva, J.C. Suarez, F.J. Ager, D. Juanes Barber, Nucl. Instrum. Methods Phys. Res. B 136 (1998) 290.
[33] F. Vera Tomé, A. Martín Sanchez, Appl. Radiat. Isot. 42 (1991) 135.
[34] C. Alonso-Hernández, M. Díaz-Asencio, A. Munos-Caravaca, E. Suarez-Morell, R. Moreno-Avila, J. Environ. Radioact. 61 (2002) 203.
[35] O.K. Hakam, A. Choukri, Z. Moutia, A. Chouak, R. Cherkaoui, J.L. Reyss, M. Lferde, Radiat. Phys. Chem. 61 (2001) 653.
[36] K. Balasubramaniam, Z. Cao Szhji, Inorg. Chem. 46 (2007) 10510.
[37] H. Huang, S. Chaudhary, J.D. Van Horn, Inorg. Chem. 44 (2005) 813.
[38] Z. Zhang, G. Helms, S.B. Clark, G. Tian, P.L. Zanonato, L. Rao, Inorg. Chem. 48 (2009) 3814.
[39] J. Dolbeault, M.J. Esteban, E. Séré, Int. J. Quantum Chem. 93 (2003) 149.
[40] E. Lenthe, E.J. Van Baerends, G. Snijders, J. Chem. Phys. 101 (1994) 9783.
[41] R. Arratia Pérez, L. Hernández Acevedo, G.L. Malli, J. Chem. Phys. 121 (2004) 7743.
[42] R. Arratia Pérez, G.L. Malli, J. Chem. Phys. (2006) 124.
[43] L. Visscher, J. Comput. Chem. 23 (2001) 759.
[44] T.A. Hopkins, J.M. Berg, D.A. Costa, W.H. Smith, H.J. Dewey, Inorg. Chem. 40 (2001) 1820.
[45] L. Seijo, Z. Barandiarán, J. Phys. Chem. 89 (1988) 5739.
[46] W. Küchle, M. Dolg, H. Stoll, H. Preuss, J. Phys. Chem. 100 (1994) 7535.
[47] M. Dolg, Mod. Algorithms Quantum Chem. 3 (2000) 507.
[48] P. Burns, Can. Mineral. 43 (2005) 1839.
[49] H.T. Evans, Science 141 (1963) 154.
[50] N. Kalsoyannis, Chem. Soc. Rev. 32 (2003) 9.
[51] J. Vázquez, C. Bo, M.J. Poblet, J. de Pablo, J. Bruno, Inorg. Chem. 42 (2003) 6136.
[52] Amsterdam Density Functional (ADF) Code, Vrije Universiteit, Amsterdam, The Netherlands, Release 2007.
[53] L. Verluis, T. Ziegler, J. Chem. Phys. 88 (1988) 322.
[54] S.H. Vosko, L. Wilk, M. Nusair, Can. J. Phys. 58 (1980) 1200.
[55] J.P. Perdew, J.A. Chevary, S.H. Vosko, K.A. Jackson, M.R. Pederson, D.J. Singh, C. Fiolhais, Phys. Rev. B: Condens. Matter 48 (1993) 4978 (Erratum Phys. Rev. B 46 (1992) 6671).
[56] R. Tagle Ramirez, R. Arratia Pérez, Chem. Phys. Lett. 475 (2009) 232.
[57] M. Cossi, B. Menucci, J. Pitarch, J. Tomasi, J. Comput. Chem. 19 (1998) 833.
[58] Ch.J. Cramer, D.G. Truhlar, Acc. Chem. Res. 42 (2009) 493.
[59] A. Klamt, B. Menucci, J. Tomasi, V. Barone, C. Curutchet, M. Orozco, F.J. Luque, Acc. Chem. Res. 42 (2009) 489.
[60] T.L. Docrat, J.F.W. Mosselmans, J.M. Charnock, M.W. Wihteley, D. Collison, F.R. Livens, C. Jones, M. Edmiston, J. Inorg. Chem. 38 (1999) 1879.
[61] P.G. Allen, J.J. Bucher, D.L. Clark, N.M. Edelstein, S.A. Ekberg, J.W. Gohdes, E.A. Hudson, N. Kaltsoyannis, W.W. Lukens, M.P. Neu, P.D. Palmer, T. Reich, D.K. Shuh, C.D. Tait, B.D. Zwick, Inorg. Chem. 34 (1995) 4797.
[62] C. Madic, D.E. Hobart, G.M. Begun, Inorg. Chem. 22 (1983) 1494.
[63] L.J. Basile, J.R. Ferraro, M.L. Mitchell, J.C. Sullivan, Appl. Spectrosc. 32 (1978) 535.
[64] L. Hemmingsen, P. Amara, E. Ansoborlo, M.J. Field, J. Phys. Chem. A 104 (2000) 4095.